Inorganic Chemistry

Article

pubs.acs.org/IC

Open-Shell Lanthanide(II+) or -(III+) Complexes Bearing σ-Silyl and Silylene Ligands: Synthesis, Structure, and Bonding Analysis

Rainer Zitz,[†] Henning Arp,[†] Johann Hlina,[‡] Małgorzata Walewska,[†] Christoph Marschner,[†] Tibor Szilvási,*[,§] Burgert Blom,*[,∥] and Judith Baumgartner*[,‡]

[†]Institut für Anorganische Chemie, Technische Universität Graz, Stremayrgasse 9, 8010 Graz, Austria

[‡]Institut für Chemie, Universität Graz, Stremayrgasse 9, 8010 Graz, Austria

[∥]Department of Chemistry: Metalorganics and Inorganic Materials, Technische Universität Berlin, Straße des 17. Juni 135, 10623 Berlin, Germany

[§]Department of Inorganic and Analytical Chemistry, Budapest University of Technology and Economics, Szent Gellért tér 4, 1111 Budapest, Hungary

Supporting Information

ABSTRACT: Complexes featuring lanthanide (Ln)−Si bonds represent a highly neglected research area. Herein, we report a series of open-shell Ln^{II+} and Ln^{III+} complexes bearing σ-bonded silyl and base-stabilized N-heterocyclic silylene (NHSi) ligands. The reactions of the Ln^{III+} complexes Cp_3Ln (Ln = Tm, Ho, Tb, Gd; Cp = cyclopentadienide) with the 18-crown-6 (18-cr-6)-stabilized 1,4-oligosilanyl dianion $[(18\text{-cr-6})KSi(SiMe_3)_2SiMe_2SiMe_2Si(SiMe_3)_2K(18\text{-cr-6})]$ (**1**) selectively afford the corresponding metallacyclopentasilane salts $[Cp_2Ln(\{Si(SiMe_3)_2SiMe_2\}_2)]^-[K_2(18\text{-cr-6})_2Cp]^+$ [Ln = Tm (**2a**), Ho (**2b**), Tb (**2c**), Gd (**2d**)]. Complexes **2a**−**2d** represent the first examples of structurally characterized Tm, Ho, Tb, and Gd complexes featuring Ln−Si bonds. Strikingly, the analogous reaction of **1** with the lighter element analogue Cp_3Ce affords the acyclic product $[Cp_3CeSi(SiMe_3)_2SiMe_2SiMe_2Si(SiMe_3)_2\text{-}Cp_3Ce]^{2-}2[K(18\text{-cr-6})]^+$ (**3**) as the first example of a complex featuring a Ce−Si bond. In an alternative synthetic approach, the aryloxy-functionalized benzamidinato NHSi ligand $Si(OC_6H_4\text{-}2\text{-}tBu)\{(NtBu)_2CPh\}$ (**4a**) and the alkoxy analogue $Si(OtBu)\{(NtBu)_2CPh\}$ (**4b**) were reacted with $Cp^*_2Sm(OEt_2)$, affording, by OEt_2 elimination, the corresponding silylene complexes, both featuring Sm^{II+} centers: $Cp^*_2Sm \leftarrow :Si(O{-}C_6H_4\text{-}2\text{-}tBu)\{(NtBu)_2CPh\}$ (**6**) and $Cp^*_2Sm \leftarrow :Si(OtBu)\{(NtBu)_2CPh\}$ (**5**). Complexes **5** and **6** are the first four-coordinate silylene complexes of any f-block element to date. All complexes were fully characterized by spectroscopic means and by single-crystal X-ray diffraction analysis. In the series **2a**−**2d**, a linear correlation was observed between the Ln−Si bond lengths and the covalent radii of the corresponding Ln metals. Moreover, in complexes **5** and **6**, notably long Sm−Si bonds are observed, in accordance with a donor−acceptor interaction between Si and Sm [**5**, 3.4396(15) Å; **6**, 3.3142(18) Å]. Density functional theory calculations were carried out for complexes **2a**−**2d**, **5**, and **6** to elucidate the bonding situation between the Ln^{II+} or Ln^{III+} centers and Si. In particular, a decrease in the Mayer bond order (MBO) of the Ln−Si bond is observed in the series **2a**−**2d** in moving from the lighter to the heavier lanthanides (Tm = 0.53, Ho = 0.62, Tb = 0.65, and Gd = 0.75), which might indicate decreasing covalency in the Ln−Si bond. In accordance with the long bond lengths observed experimentally in complexes **5** and **6**, comparatively low MBOs were determined for both silylene complexes (**5**, 0.24; **6**, 0.25) .

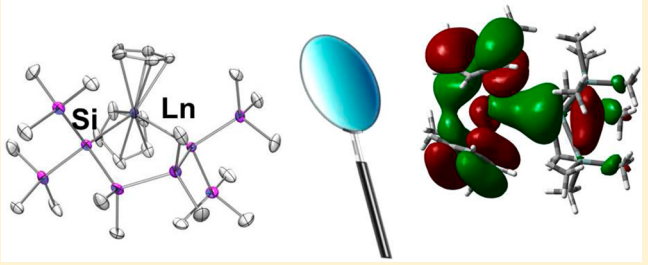

INTRODUCTION

Compounds featuring lanthanide (Ln)−Si bonds are somewhat rare in contemporary literature,[1−3] further highlighted by the fact that, for the elements Ce, Tb, and also Pm, no examples exist. Sm and the late lanthanide metals Yb and Lu are the best-studied elements for this class of compounds, with several reported examples. Arguably, the most straightforward synthesis of lanthanide silyl compounds was described in the seminal work of Bochkarev and co-workers,[4] who obtained neutral $(Ph_3Si)_2Yb^{II}(THF)_4$ directly from elemental Yb and Ph_3SiCl in tetrahydrofuran (THF; eq 1).

$$2Ph_3SiCl + 2Yb \xrightarrow{THF} (Ph_3Si)_2Yb(THF)_4 + YbCl_2(THF)_2 \quad (1)$$

Utilizing a common method for the preparation of early-transition-metal complexes, Schumann and co-workers carried out salt elimination reactions of rare-earth halide complexes with Me_3SiLi. Reactions with $Cp_2Ln(\mu\text{-}Cl)_2Na$ in 1,2-dimethoxyethane (DME) led to the respective ate complexes of the type $[Li(DME)_3][Cp_2Ln(SiMe_3)_2]$ for Ln = Sm,[5,6]

Received: December 17, 2014
Published: March 10, 2015

DOI: 10.1021/ic502991p
Inorg. Chem. 2015, 54, 3306−3315

Lu,[5−7] Dy,[7] Ho,[7] Er,[7] and Tm[7] (eq 2). More recently, Sgro and Piers reported the synthesis of gadolinium silyl complexes by reacting a potassium silanide with GdI_3.[8]

$$Cp_2LnCl{\cdot}NaCl{\cdot}2DME + 2LiSiMe_3 \xrightarrow[Ln=Sm,Lu]{} NaCl + LiCL + [Li(DME)_3] + [Cp_2Ln(SiMe_3)_3]_2 \quad (2)$$

In close analogy, Tilley and co-workers obtained the neutral Sc complexes $Cp_2Sc(SiR_3)(THF)$ from $[Cp_2ScCl]_2$ and a series of larger lithium silanides.[9] In a related reaction, Lawless and co-workers found that conversion of $[Cp^*_2Yb(OEt_2)]$ with $LiSi(SiMe_3)_3$ in THF afforded the ytterbium silyl $[Cp^*Yb^{II}(Si(SiMe_3)_3)(THF)_2]$ with concomitant elimination of $LiCp^*$.[10] Other examples of Cp_2Ln^{II} silyl complexes were obtained, with the likely involvement of silyl anions from the reaction of $Cp^*_2Ln(THF)_2$ (Ln = Sm, Eu, Yb) with $PhSiH_3$/KH, which yielded $K[Cp^*_2Ln^{II}(SiH_3)(THF)]$.[11] In the latter complex, the K ion coordinates to two Cp* ligands of different molecules, one THF moiety, and even to the SiH_3 ligand, forming a two-dimensional-layered structure in the solid state.[12] The Cp*K unit thus serves as a neutral stabilization ligand for Ln^{II} complexes otherwise intractable and difficult to isolate.

Alternatively, a number of rare-earth silyl compounds have been obtained by σ-bond metathesis routes in reactions of rare-earth alkyl complexes with hydrosilanes. Reactions of $Cp^*_2LnCH(SiMe_3)_2$ with neat $H_2Si(SiMe_3)_2$ gave neutral $Cp^*_2LnSiH(SiMe_3)_2$ (Ln = Sm, Nd, Y),[13−15] described as extremely air- and moisture-sensitive but thermally stable in solution and in the solid state. The use of a high excess of silane was found necessary for suppression of thermal decomposition of $Cp^*_2LnCH(SiMe_3)_2$. When $Cp^*_2SmCH(SiMe_3)_2$ was treated with $PhSiH_3$ instead of a bulky hydrosilane (in benzene), a number of interesting cluster compounds were obtained, all of which included three Cp^*_2Sm units and different silyl ligands (bridging SiH_2 and SiH_3 groups) bearing no phenyl groups.[15,16] The same reaction in pentane led to trimeric $Cp^*_2SmSiH_3$, which was found to be an intermediate in the cluster formation.[17,18] Reaction of o-$MeOC_6H_4SiH_3$ with $[Cp^*Lu(\mu\text{-}H)]_2$ led to the neutral lutetium silyl complex $Cp^*LuSiH_2(o\text{-}MeOC_6H_4)$.[19]

Reactions of the thermally stable N-heterocyclic silylene (NHSi) $Si[\{N(CH_2tBu)\}_2C_6H_4]$ (Si[NN]) and Cp_3Ln (Ln = Y, Yb) led to the first group 3 (Y) and lanthanide (Yb) metal silylene complexes $Cp_3LnSi[NN]$[20] (eq 3). Under similar

$$Cp_3Ln + Si[NN] \underset{Ln = Y,\ Yb}{\rightleftharpoons} Cp_3LnSi[NN] \quad (3)$$

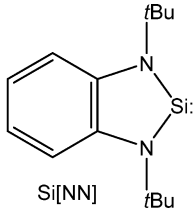

reaction conditions, Cp_3La turned out to be unreactive. Evans and co-workers reported the reaction of Cp^*_2Sm with West's stable silylene, and a Sm^{II}−Si^{II} complex was obtained.[21] That the nature of the interaction between Sm and Si is likely to be of the donor−acceptor type was shown by the fact that the silylene ligand could easily be displaced by THF, but no further studies were carried out in this direction, nor was any detailed bonding analysis carried out to date.

Inspired by this seminal work and as an extension of our recent studies on the chemistry of disilylated group 4 metallocenes[22,23] with the oxidation state 3+, we decided to explore this neglected area of Ln chemistry, with a view of systematically studying the nature of the La−Si bond for both Ln^{II+} and Ln^{III+} complexes. Herein we report a novel and facile synthetic route to a range of σ-bonded lanthanide silyl complexes in the III+ oxidation state, as well as novel samarium(II+) silylene complexes. A rigorous investigation into their spectroscopic properties and structures by X-ray diffraction (XRD) studies and the first systematic density functional theory (DFT) investigation for this class of complexes are reported.

RESULTS AND DISCUSSION

Synthesis. Reactions of the readily accessible metallocenes (Cp_3Ln) of the elements Gd, Tb, Ho, and Tm with the 1,4-oligosilanyl dianion **1**[24,25] afford cleanly the corresponding metallacyclopentasilane ate complexes (**2a−2d**) with the Ln metals in the oxidation state 3+ together with $[\{K(18\text{-cr-}6)\}_2Cp]^+$ (where 18-cr-6 = 18-crown-6) as the counterion (Scheme 1). The ease of access to these complexes prompted us to explore the reaction with (Cp_3Ce), a lighter analogue of the heavier lanthanides. Contrary to the other used metallocenes (Cp_3Ln), Cp_3Ce is not commercially available but can readily be synthesized.[26] Reaction of dianion **1** with Cp_3Ce did not lead to a five-membered ring but to the acyclic compound **3** (Scheme 1), which to the best of our knowledge is the first example of a compound featuring a Si−Ce bond. Each Ce^{III} atom retains all of its three Cp ligands while forming an additional Ce−Si bond. One of the Cp ligands on each Ce coordinates to the cationic moiety K(18-cr-6)·THF. All complexes **2a−2d** and **3** are thermally stable but extremely sensitive to moisture and air, as expected for organometallic Ln complexes.

In addition to these lanthanide silyl complexes, we are also interested in the synthesis of base-stabilized silylene lanthanide metal complexes because instead of featuring a σ-bonded silyl group they would rather exhibit coordinative (donor−acceptor) bonds between Si and the Ln element, which would be of interest as a comparison. As a starting point, we decided to investigate the reactivity of $Cp^*_2Sm(OEt_2)$, which is readily available,[27] toward NHSi ligands. Given the robust coordination of Roesky's chlorosilylene $Si(Cl)[(NtBu)_2CPh]$ (**4**) toward a range of transition metals,[28] we first explored its reaction with $Cp^*_2Sm(OEt_2)$. Reaction of $Cp^*_2Sm(OEt_2)$ with silylene **4**,[29,30] in fact, produced an inseparable mixture of the "interconnected" silylene(I) dimer LSi−SiL[31] and the Sm^{III} complex Cp^*_2SmCl rather than the desired coordination complex, based on multinuclear NMR spectroscopy and comparison to authentic samples of both complexes. Clearly, redox chemistry dominates this reaction and precludes the isolation of the desired NHSi complex. To circumvent this problem, **4** was functionalized by replacement of the Cl atom at Si by an aryloxy (**4a**),[32] or alkoxy group (**4b**),[33] reasoning that the increased bond strength of Si−O versus Si−Cl could suppress this redox chemistry and thus facilitate formation of the desired NHSi coordination complex. This was indeed the case, and the silylene complexes **5** and **6** could be isolated in moderate-to-good yields (Scheme 2). Complexes **5** and **6** represent the first examples of isolated four-coordinate silylene complexes of any f-block element.

DOI: 10.1021/ic502991p
Inorg. Chem. 2015, 54, 3306−3315

Scheme 1. Preparation of Lanthanide Oligosilanyl Complexes 2a−2d and 3

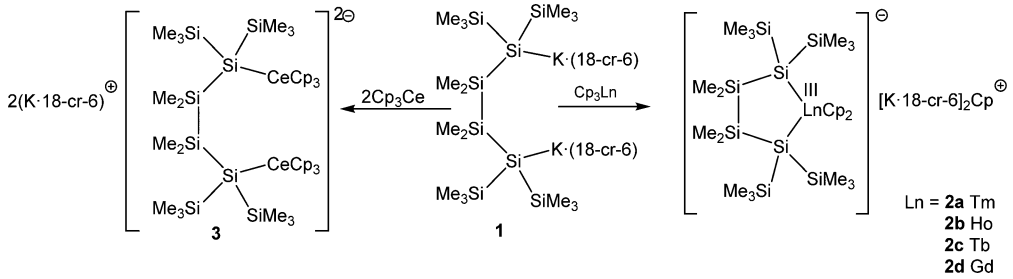

Scheme 2. Synthesis of Samarium Silylene Complexes 5 and 6

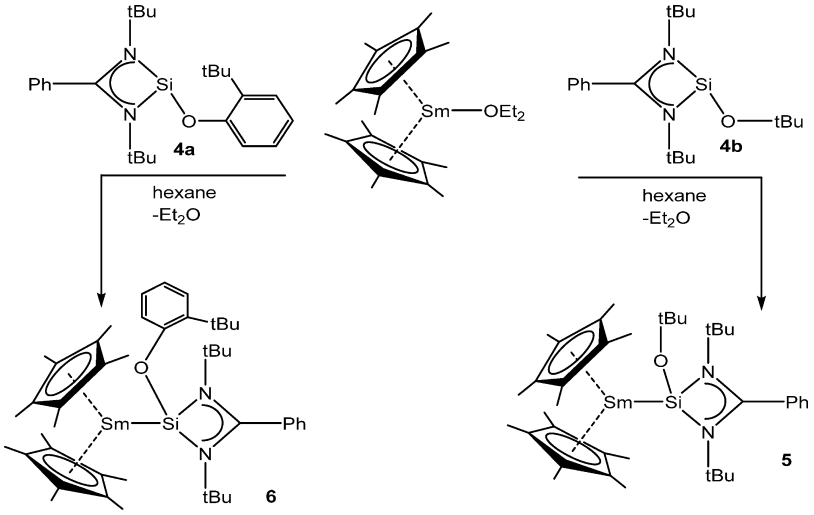

The dinuclear mixed-valent complex **7** (Scheme 3), featuring Sm^{II} and Sm^{III} bridged by a μ-iodide ligand, was coincidentally

Scheme 3. Plausible Formation of 7 from 5

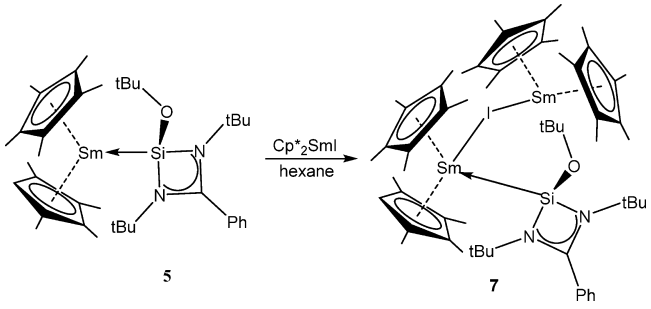

isolated as a minor byproduct of the supernatant solution from the reaction mixture of complex **5**. Presumably, its formation stems from trace amounts of Cp^*_2SmI, present in the starting material $Cp^*_2Sm(OEt_2)$, upon reaction with **5**. Unfortunately, only a few crystals were obtained, which precluded further spectroscopic characterization, but nevertheless it is an interesting complex from a structural point of view.

Complexes **5** and **6** are paramagnetic, with magnetic moments μ_{eff} = 2.7 μ_B (**5**) and 2.6 μ_B (**6**) (Evans' method).[34] This is dramatically reduced upon comparison to the Sm^{II} starting material $Cp^*_2Sm(OEt_2)$ (μ_{eff}= 3.6 μ_B) possibly because of the NHSi ligands affecting spin−orbit coupling in the Sm center. This suggests that the NHSi ligand influences the magnetic properties of the emerging Sm^{II} complexes considerably, which is likely attributable to the different nature of the Si: → coordination versus the O: → coordination of Et_2O in $Cp^*_2Sm(OEt_2)$.

NMR Spectroscopy. NMR spectroscopic characterization of open-shell Ln complexes is somewhat challenging, particularly because of spin−orbit coupling phenomena. These properties have been exploited in Ln shift reagents.[35,36] Diamagnetic complexes, however, also exist and possess either f^0 (La^{III} and Ce^{IV}) or f^{14} (Lu^{III} and Yb^{II}) electron configurations.

Nevertheless, even for the respective lanthanide metallocene complexes, investigations started early on,[37] and currently chemical shifts for a substantial number of lanthanide metallocene complexes are known. It is important to note that while there are certainly trends governing the chemical shift behavior, their interpretation is not straightforward. The chemical shifts of protons attached directly to cyclopentadienyl ligands are frequently dramatically different from the shifts observed for methyl groups on cyclopentadienyl ligands (see below).

A short survey on the existing NMR characterization data for Cp_2Ln, Cp_2LnL, Cp_2LnX, Cp_3Ln, and related complexes [such as $CpMe_n$, $Cp(SiMe_3)_n$, etc.] of Ce, Sm, Tm, Tb, Ho, and Gd reveals numerous examples for Sm and Ce, while there are only scant examples for Tm,[7,38−42] Tb,[7,37,43,44] Ho,[7,37,45] and Gd.[7,44,46−50] Furthermore, it should be noted that usually only ^{1}H NMR data are given, but ^{29}Si or even ^{13}C NMR data are neglected.

Comprehensive studies dealing with the magnetic effects of certain electronic configurations on the chemical shift behavior of ligands are extremely rare. For silylated complexes, the seminal work of Schumann and co-workers compared ^{1}H NMR resonances of a number of complexes of the type $Cp_2Ln(\mu$-

DOI: 10.1021/ic502991p
Inorg. Chem. 2015, 54, 3306−3315

$Cl)_2Na{\cdot}DME$ (Ln = Sm, Gd, Tb, Dy, Ho, Er, Tm, Lu) versus $[Li{\cdot}DME_n]Cp_2Ln(SiMe_3)_2$ (Ln = Sm, Dy, Ho, Er, Tm, Lu).[7] Inspection of the chemical shifts in this series reveals that, in particular, the Cp−H resonances of Tb^{III} and Ho^{III} are strongly downfield-shifted to values close to 160 ppm, whereas the respective signals of Er^{III} and Tm^{III} are considerably upfield-shifted to values of around −60 ppm. Extremely shifted resonances of the $SiMe_3$ groups were found for Ho^{III} and Er^{III}. The sign of the magnetically induced shift of the $SiMe_3$ resonance is, however, reversed compared to that of the Cp resonance.[7]

For compounds **2a**−**2d**, we recorded ^{1}H NMR spectra (Table 1). It is important to consider the fact that not only are

Table 1. ^{1}H NMR Data of Compounds 2a−2d (Solvent: THF-d_8)

compound	^{1}H: *Cp*Ln	^{1}H: Si*Me*$_3$	^{1}H: Si*Me*$_2$
2a (Tm)	−48.30	16.71	−11.93
2b (Ho)	−22.41	1.58	1.66
2c (Tb)	−24.32	0.63	0.72
2d (Gd)	9.23	2.35	2.20

NMR spectra of Ln compounds paramagnetically shifted and generally exhibit line-broadening, but chemical shifts are frequently also concentration- and temperature-dependent.[51] Nuclei with reduced natural abundance are therefore frequently difficult to detect. Nevertheless, for compounds **2b**−**2d**, it was possible to measure two-dimensional ^{1}H−^{13}C and ^{1}H−^{29}Si correlation NMR spectra at room temperature, which was indispensable for the assignments of the signals.

It is instructive to compare the ^{1}H chemical shifts recorded for **2a**−**2d** to those observed for the complexes of Schumann. The behavior of complex **2a** was indeed very similar to what had been observed for Schumann's compound $[Cp_2Tm(SiMe_3)_2]^-$. The Cp resonance of **2a** at −48.3 ppm is close to $[Cp_2Tm(SiMe_3)_2]^-$ at −56.7 ppm. A comparison similar to Schumann's Ho compound, however, shows a completely different picture. While the CpH resonance for $[Cp_2Ho(SiMe_3)_2]^-$ was described at very low field (164.2 ppm), we observed the analogous resonance of **2b** at −22.4 ppm. It should, however, be noted that the number of NMR spectroscopically characterized Cp_nHo^{III} compounds is rather limited,[7,37,45] and therefore it is difficult to assess the observed chemical shift values. Compared to the Cp resonances, the SiMe signals are found to exhibit comparably normal chemical shifts. Considering the fact that the shift caused by the paramagnetic atoms decreases with $1/r^3$, it can be expected that more remote atoms experience a much smaller shifting effect. Only for complex **2a**, which also exhibits a very strong effect on the CpH resonances (−48.3 ppm), also the $SiMe_3$ resonances are severely shifted to 16.7 ppm. With respect to the ^{29}Si NMR data, we were able to obtain values for compounds **2b**−**2d** (Table 2). The values of **2b** and **2c** are quite similar, which is consistent with Schumann's proton NMR study where Ho and Tb showed similar shift behavior. The values for the $SiMe_3$ resonance of the Gd compound **2d** are also in line with those observed for **2b** and **2c**. The resonance detected for the $SiMe_2$ units is, however, clearly different.

Strikingly, for the silylene complexes **5** and **6** both featuring Sm^{II+} centers, in the respective ^{1}H NMR spectra, most of the signals are observed in the diamagnetic spectral window, at odds with the complexes discussed above. Noteworthy,

Table 2. ^{29}Si NMR Data of Compounds 2b−2d (Solvent: THF-d_8)

compound	^{29}Si: *Si*Me$_3$	^{29}Si: *Si*Me$_2$	^{29}Si: *Si*$_q$
2b (Ho)	−9.0	−35.2	−114.9
2c (Tb)	−10.6	−36.1	−116.3
2d (Gd)	−7.7	−1.4	n.d.[a]

[a]n.d. = not detected.

however, are dramatic shifts of the aryl protons in both complexes, to both high- and low-field regions, because of the paramagnetic influence of the Sm^{II} center (Figure 1). Some of

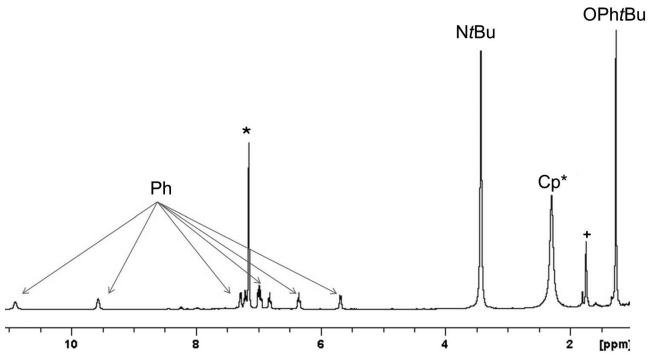

Figure 1. ^{1}H NMR spectrum of complex **6** in C_6D_6 at 298 K: (*) C_6D_5H; (+) trace impurity. The high- and low-field chemical shift positions of the aryl protons are indicated.

the signals are also somewhat line-broadened. The ^{13}C NMR spectra for both complexes also reveal most of the signals in the expected diamagnetic spectral range, some again somewhat line-broaded, although the resonance signals corresponding to the ring atoms of the coordinated Cp* ligand could not be observed in both complexes, akin to the Cp complexes described above.

Two-dimensional HSQC and HMBC correlation experiments were also carried out for complexes **5** and **6** for an unambiguous assignment of the ^{13}C NMR signals. Because of the paramagnetic nature of the complexes, although cross peaks were observed in alignment with the signals in the ^{1}H NMR spectrum, these did not correspond to any observable signals in the ^{13}C NMR spectra, in both cases. This suggests that the routine pulse sequence for these traditional two-dimensional correlation experiments is not appropriate for the Sm^{II} complexes, although with the Ln^{III} complexes described above, it was possible. Moreover, despite extremely long (ca. 72 h) acquisition periods, at high concentrations, no signals could be observed in the ^{29}Si NMR spectra because of the paramagnetic influence of the Sm^{II} center.

X-ray Crystallography. Single-crystal structure analyses could be carried out for all new compounds (**2a**−**2d**, **3**, and **5**−**7**). The isostructural compounds **2a**, **2b**, and **2d** (Figure 2) crystallized in the monoclinic space group $P2(1)/n$, except the Tb compound **2c** ($P\bar{1}$) because of the four THF molecules in the asymmetric unit.

In all four structures, the ion pairs are separated. The countercation (18-cr-6)K-Cp-K(18-cr-6) shows disorder in one crown ether for **2b** and in both crown ethers for **2a** and **2d**, a fact that is reflected by the number of restraints used. The Ce complex **3** (Figure 3) crystallized in the triclinic space group $P\bar{1}$ with an additional toluene molecule in the asymmetric unit.

DOI: 10.1021/ic502991p
Inorg. Chem. 2015, 54, 3306−3315

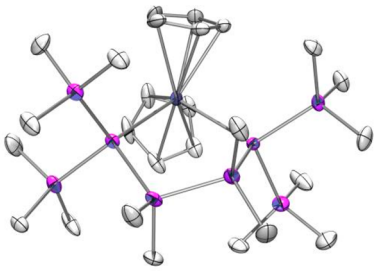

2a	2b	2c	2d
slight yellow crystals	yellow crystals	slight yellow crystals	slight yellow crystals
space group: P2(1)/n	space group: P2(1)/n	space group: P-1 (+4THF)	space group: P2(1)/n
Si-Tm: 2.965, 2.980 Å	Si-Ho: 2.986, 2.999 Å	Si-Tb: 3.018, 3.020 Å	Si-Gd: 3.018, 3.037 Å
Si-Tm-Si: 94.15°	Si-Ho-Si: 94.68°	Si-Tb-Si: 95.47°	Si-Gd-Si: 94.84°

Figure 2. Some key metrical parameters from the crystal structures of the isostructural complexes **2a**–**2d**. Thermal ellipsoids are at the 30% probability level and hydrogen atoms omitted for clarity. Color code: purple ellipsoid, Ln metal [Tm (**2a**), Ho (**2b**), Tb (**2c**), Gd (**2d**)]; pink ellipsoid, silicon; light gray, carbon.

One of the Cp ligands coordinates to the cationic moiety K/18-cr-6/THF.

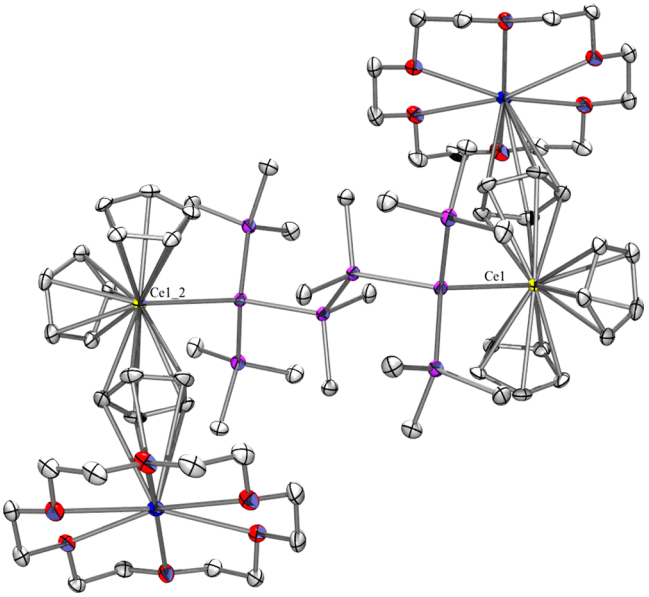

Figure 3. Molecular structure of **3** (thermal ellipsoid plot drawn at the 30% probability level). All hydrogen atoms are omitted for clarity. Bond lengths (Å) and angles (deg): Ce1–C1 2.817(3), Ce1–C6 2.844(3), Ce1–Si1 3.2283(2), Si1–Si4 2.3601(15), Si1–Si3 2.3784(13), Si1–Si2 2.3981(13); Si4–Si1–Si3 99.54(5), Si4–Si1–Si2 102.43(6), Si3–Si1–Si2 98.81(5), Si4–Si1–Ce1 115.26(5), Si3–Si1–Ce1 111.43(4), Si2–Si1–Ce1 125.37(5).

The cyclopentadienyl rings in all five compounds are bonded in η^5 fashion with increasing bond lengths between the centroids of the Cp rings and the lanthanoid atoms: in **2a** (Tm) 2.335 and 2.328 Å, in **2b** (Ho) 2.363 and 2.349 Å, in **2c** (Tb) 2.401 and 2.388 Å, in **2d** (Gd) 2.401 and 2.394, and finally in **3** (Ce) 2.565 and 2.562 Å. These distances (Cp ring centroid–metal) are in good agreement with comparable Cp_2Ln^{III} compounds (Tm,[38] Ho,[52–54] Tb,[44,55,56] Gd,[57–59] and Ce[53,60,61]). The Cp–Ce distance in **3**, where the K atoms are coordinated to the Cp rings, is 2.581 Å slightly elongated.

Because **2a**–**2d** and **3** are the first structurally characterized complexes bearing a Ce–Si, Tm–Si, Ho–Si, Tb–Si, or Gd–Si bond, no data for comparison are available. The most striking features of these molecular structures are the values for the lanthanide–silyl bond lengths, which are in good agreement with the sum of the covalent radii (Figure 4).[62] The distances

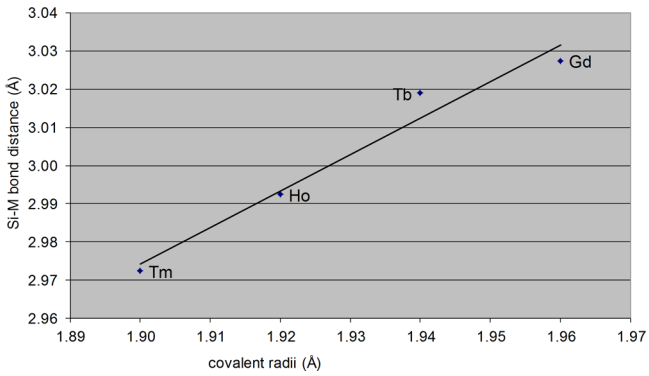

Figure 4. Plot of Si–M (M = Tm, Ho, Tb, Gd) versus covalent radii.[62] Si–M is the average bond length in **2a**–**2d**.

between Ln and Si decrease incrementally with decreasing metal size, as expected. This indicates that the Ln–Si bond is rather polar but might possess at least some covalent character.[63] The bond angle Si–Ln–Si varies only slightly from 94.15° in **2a** (Tm) to 94.68° in **2b** (Ho) to 95.47° in **2c** (Tb) to 94.84° in **2d** (Gd).

Compound **5** (Figure 5) crystallized in the monoclinic space group $P2(1)/n$, **6** (Figure 6) in orthorhombic $P2(1)2(1)2(1)$,

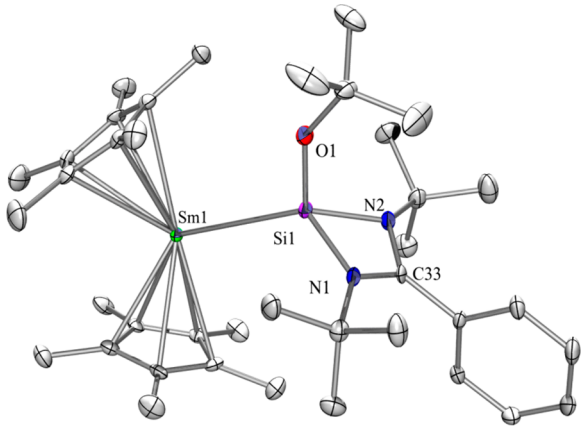

Figure 5. Molecular structure of **5** (thermal ellipsoid plot drawn at the 30% probability level). All hydrogen atoms are omitted for clarity. Bond lengths (Å) and angles (deg): Sm1–C19 2.772(6), Sm1–C12 2.853(6), Sm1–Si1 3.4396(15), Si1–O1 1.645(4), Si1–N1 1.875(5), Si1–N2 1.876(5); O1–Si1–N1 107.6(2), O1–Si1–N2 107.2(2), N1–Si1–N2 68.9(2), O1–Si1–Sm1 114.23(16), N1–Si1–Sm1 128.16(16), N2–Si1–Sm1 122.14(18).

and **7** (Figure 7) in triclinic $P\bar{1}$ with two benzene molecules and two additional ones on special positions in the unit cell. The Sm–Si distance for the samarium silylene synthesized by Evans et al.[21] is 3.192 Å. The Sm–Si distances for our compounds are with 3.440 Å for **5**, 3.314 Å for **6**, and 3.299 Å for **7** substantially longer, suggesting a weaker interaction.

The Si–Sm bond length in **7** is 3.299 Å, shorter by 0.141 Å compared to that in the starting material **5**. The Sm^{III}–I

DOI: 10.1021/ic502991p
Inorg. Chem. 2015, 54, 3306–3315

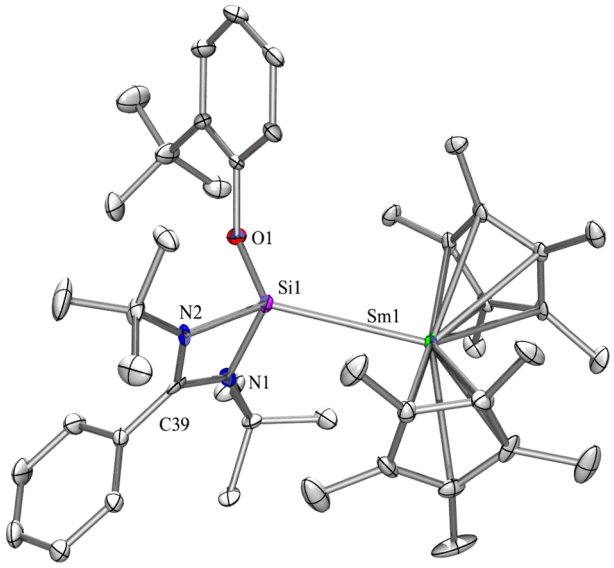

Figure 6. Molecular structure of **6** (thermal ellipsoid plot drawn at the 30% probability level). All hydrogen atoms are omitted for clarity. Bond lengths (Å) and angles (deg): Sm1–Si1 3.3142(18), Si1–O1 1.683(7), Si1–N1 1.865(7), Si1–N2 1.872(7); O1–Si1–N1 96.8(3), O1–Si1–N2 100.0(3), N1–Si1–N2 69.7(3), O1–Si1–Sm1 125.2(2), N1–Si1–Sm1 107.9(2), N2–Si1–Sm1 134.2(2).

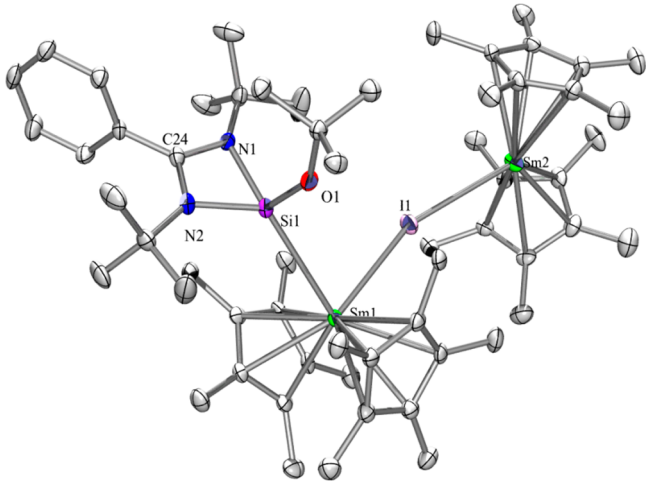

Figure 7. Molecular structure of **7** (thermal ellipsoid plot drawn at the 30% probability level). All hydrogen atoms are omitted for clarity. Bond lengths (Å) and angles (deg): Sm1–I1 3.1069(6), Sm1–Si1 3.2992(18), Sm2–I1 3.2962(7), N1–Si1 1.888(5), N2–Si1 1.884(6), O1–Si1 1.626(5); I1–Sm1–Si1 89.80(3), Sm1–I1–Sm2 160.89(2), O1–Si1–N2 108.4(3), O1–Si1–N1 108.3(3), N2–Si1–N1 70.0(2), O1–Si1–Sm1 106.61(17), N2–Si1–Sm1 130.7(2), N1–Si1–Sm1 128.09(19).

distance of **7** is 3.107 Å, and Sm^{II}–I is 3.296 Å, slightly longer, with a Sm^{III}–I-Sm^{II} angle of 160.83°. The value for the Sm^{III}–I distance is in good comparison to those of three published structures (3.044 Å,[64] 3.100 Å,[65] and 3.180 Å[66]). Because no dinuclear Sm complexes with two different oxidation states are reported in the literature, a comparison is not possible. Most reported complexes containing the Sm–I–Sm unit are dimers of samarium iodides featuring four-membered Sm–I–Sm–I rings; the Sm–I–Sm angles are therefore close to 100°, and only one example is given for a six-membered ring system featuring alternate Sm^{III} and I atoms with a Sm–I–Sm angle of 154.43°.[66] The Cp* centroid–Sm–Cp* centroid angle is 134.91° in **5**, 140.19° in **6**, and 133.29° (Sm1) and 139.74° (Sm2) in **7**, similar to 138.5° reported for the samarium silylene by Evans and co-workers.[21] In the latter compound, the silylene ligand is bent in a way that the two *N-tert*-butyl groups have different distances to the Sm atom and different Sm–Si–N angles (118.2° and 150.8°). In compounds **5** and **7**, these angles are just slightly different (122.1° and 128.2° for **5** and 130.7° and 128.1 for **6**), and only in **6**, the difference is more pronounced with 107.9° and 134.2°.

DFT Calculations. The electronic structures of synthesized complexes (**2a–2d**, **5**, and **6**) at the B3PW91/Basis1 level of theory were calculated. According to these calculations, the Tm–Si bond distances (2.958 and 2.971 Å) in the optimized geometry of **2a** show perfect agreement with the experimentally characterized distances (2.966 and 2.980 Å, respectively). Natural bond orbital (NBO) analysis suggests that the negative charge of **2a** is mainly localized on the Si atoms (−0.25) connected to the Tm center (Table 3), whereas other Si atoms show large positive natural population between 0.3+ and 0.55+. In addition, NBO analysis shows lone pairs on the Si atoms. Interestingly, the shape of the highest occupied molecular orbital (HOMO) and HOMO−1 exhibits some covalent and ionic character bonding as well. The HOMO (−0.54 eV) depicted in Figure 8 shows a lone pair on the Si center, which can be interpreted in light of the negative charge of **2a** as a bond with strongly polarized or even ionic character where the Si bears the two electrons. In contrast to that, HOMO−1 (−0.86 eV) denotes more covalent character because the orbital is extended toward the Tm center as well. This also agrees with the Mayer bond order (MBOs) that supports the picture of weak, very polarized bonds (0.53).

Table 3. Calculated Average Ln–Si Bond Lengths (Å), MBOs of Ln–Si Bonds, Natural Population Analysis Charges, and HOMO Energies (eV) for 2a–2d, 5, and 6 at the B3PW91/Basis 1 Level of Theory

compound	Ln–Si bond distance (Å)	MBO of Ln–Si bonds	NPA charge (Ln/Si)	HOMO energy (eV)
2a (Tm)	2.965	0.53	+2.28/−0.25	−0.54
2b (Ho)	2.996	0.62	+2.41/−0.21	−0.66
2c (Tb)	3.017	0.65	+2.35/−0.23	−0.86
2d (Gd)	3.028	0.75	+2.27/−0.22	−0.77
5 (Sm)	3.411	0.24	+1.99/+1.50	−1.67
6 (Sm)	3.278	0.25	+2.01/+1.66	−1.72

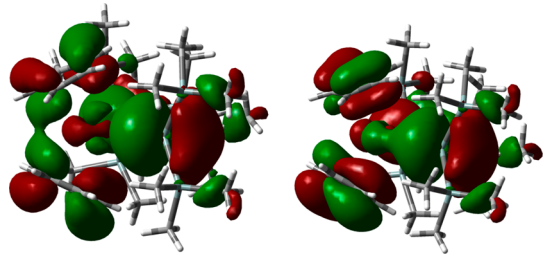

Figure 8. HOMO (left) and HOMO−1 (right) of **2a** calculated at the B3PW91/Basis1 level of theory (isovalue: 0.02). White, gray, blue, and teal refer to H, C, Tm, and Si atoms, respectively.

The analogous Gd complex, **2d**, features a half-filled f shell ($S = {}^{7}/_{2}$), and the Gd–Si bond distances (3.025 and 3.030 Å) in

DOI: 10.1021/ic502991p
Inorg. Chem. 2015, 54, 3306–3315

the optimized geometry also show agreement with the experimentally characterized distances (3.018 and 3.038 Å, respectively). HOMO (−0.77 eV) and HOMO−1 (−0.97 eV) (Figure 10) depict more covalent character than that in the case of **2a** because HOMO−1 exhibits uniform extension between the Gd and Si atoms. MBOs of Gd−Si bonds (0.73 and 0.75) are larger than that of Tm−Si bonds (0.53), although NBO analysis still suggests lone pairs on the Si atoms. For **2b** and **2c**, the calculated bond distances, bond orders, and charges (Table 3) are between the discussed theoretical results of **2a** and **2d**; therefore, the calculated parameters follow the experimentally characterized series of bond lengths, providing further evidence of the partial covalent character of the Ln−Si bonds as HOMO and HOMO−1 also suggest (Figures 9−11). The calculated

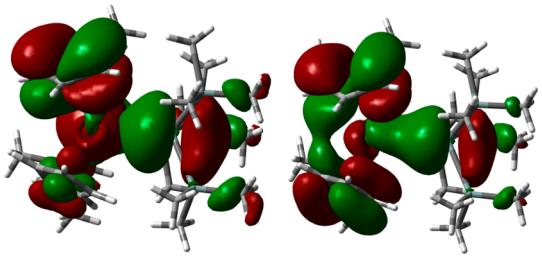

Figure 9. HOMO (left) and HOMO−1 (right) of **2b** calculated at the B3PW91/Basis1 level of theory (isovalue: 0.02). White, gray, blue, and teal refer to H, C, Ho, and Si atoms, respectively.

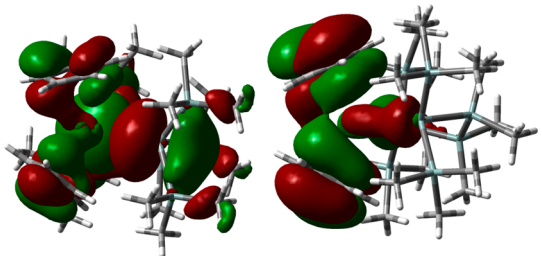

Figure 10. HOMO (left) and HOMO−1 (right) of **2d** calculated at the B3PW91/Basis1 level of theory (isovalue: 0.02). White, gray, blue, and teal refer to H, C, Gd, and Si atoms, respectively.

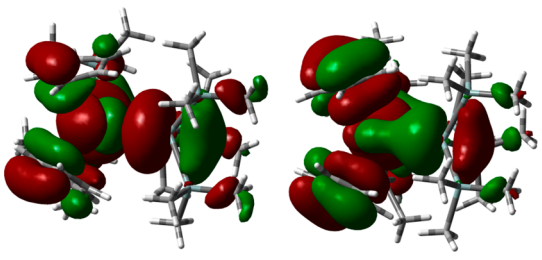

Figure 11. HOMO (left) and HOMO−1 (right) of **2c** calculated at the B3PW91/Basis1 level of theory (isovalue: 0.02). White, gray, blue, and teal refer to H, C, Tb, and Si atoms, respectively.

data in the series of **2a**−**2d** might also indicate, in agreement with the previously suggested relationship of bond lengths, some covalency in the bonding character (Figure 4).[39]

Samarium silylene complexes (**5** and **6**) have triplet ground states in accordance with the Evans magnetometric measurements. The calculated structures are in moderate agreement with the experimentally characterized geometries; the calculated Sm−Si distances are somewhat shorter (3.411 and 3.278 Å, respectively; Table 3) than the experimental values (3.440 and 3.315 Å, respectively). In spite of the shorter Sm−Si distance, none of the applied methods suggests considerable covalent character of the Sm−Si bond, which is in good agreement with the relatively large bond distances. NBO analysis displays a lone pair on the Si centers because the HOMOs of **5** and **6** exhibit the same (Figure 12) features. MBOs indicate very low bond order of 0.24 and 0.25 for **5** and **6**, respectively.

CONCLUSION AND SUMMARY

In summary, a range of novel open-shell Ln complexes in the II + or III+ oxidation state bearing σ-bonded silyl groups or coordinated NHSi ligands have been reported, characterized spectroscopically and by structural means, and further elucidated by DFT methods. The σ-bonded silyl complexes feature Ln−Si bonds with much higher MBO indices compared to the LnSi complexes bearing coordinated NHSi ligands. A general trend is a decrease in the covalent nature of the Ln−Si bond for complexes $[Cp_2Ln(\{Si(SiMe_3)_2SiMe_2\}_2)]^-[(K18\text{-}cr\text{-}6)_2Cp]^+$ [Ln = Tm (**2a**), Ho (**2b**), Gd (**2c**), Tb (**2d**)] on moving from left to right across the lanthanides, as evidenced by an incremental decrease in the MBOs. The ease of synthetic access to these open-shell complexes featuring Ln−Si bonds highlighted herein is of fundamental importance and potentially opens the door to further fundamental investigations of these hitherto poorly investigated complexes.

EXPERIMENTAL SECTION

General Remarks. All reactions involving air-sensitive compounds were carried out under an atmosphere of dry nitrogen or argon using either Schlenk techniques or a glovebox. All solvents were dried using a column-based solvent purification system.[67] Chemicals were obtained from different suppliers and used without further purification. Silyl dianion **1**,[24,25] Cp_3Ce,[26] $Cp^*_2Sm(OEt_2)$,[27] and ligands **4a**[32] and **4b**[33] were prepared following reported procedures.

^1H (300 MHz), ^{13}C (75.4 MHz), and ^{29}Si (59.3 MHz) NMR spectra were recorded on a Varian INOVA 300 spectrometer or on Bruker spectrometers (AV400 or AV200). To compensate for the low isotopic abundance of ^{29}Si, the INEPT pulse sequence was used where possible for amplification of the signal.[68,69] To obtain reliable ^1H, ^{13}C, and ^{29}Si NMR shifts, samples with tetramethylsilane (TMS) added were used to obtain a reference point. ^1H Cp signals could only be observed with more concentrated samples that were referenced using the shifts obtained from the dilute spectra. gHMBC $^1H-^{29}Si$ experiments (without TMS added) were carried out to determine all ^{29}Si NMR shifts. To rule out measurement of the most plausible side product 1,1,2,2-tetrakis(trimethylsilyl)tetramethylcyclotetrasilane, which might resonate at different chemical shifts because of paramagnetic interaction, several of the gHMBC $^1H-^{29}Si$ experiments were repeated with the deliberate addition of 1,1,2,2-tetrakis-(trimethylsilyl)tetramethylcyclotetrasilane, exhibiting the expected additional set of signals.

High-resolution (HR) electrospray ionization mass spectrometry (ESI-MS) spectra were recorded on an Orbitrap LTQ XL of a Thermo Scientific mass spectrometer and the raw data evaluated using the *Xcalibur* computer program. UV spectra were measured on a PerkinElmer Lambda 35 spectrometer using spectroscopic grade pentane as the solvent.

X-ray Structure Determination. For X-ray structure analyses, the crystals were mounted onto the tip of glass fibers. Data collection was performed with a Bruker-AXS SMART APEX CCD diffractometer using graphite-monochromated Mo Kα radiation (0.71073 Å) for **2a**−**2d** and **3** and on an Agilent Technologies SuperNova (single source, Cu Kα radiation, λ = 1.5418 Å) for **5**−**7**. The data were reduced to F_o^2 and corrected for absorption effects with *SAINT*[70] and *SADABS*,[71,72] respectively. The structures were solved by direct methods and refined

DOI: 10.1021/ic502991p
Inorg. Chem. 2015, 54, 3306−3315

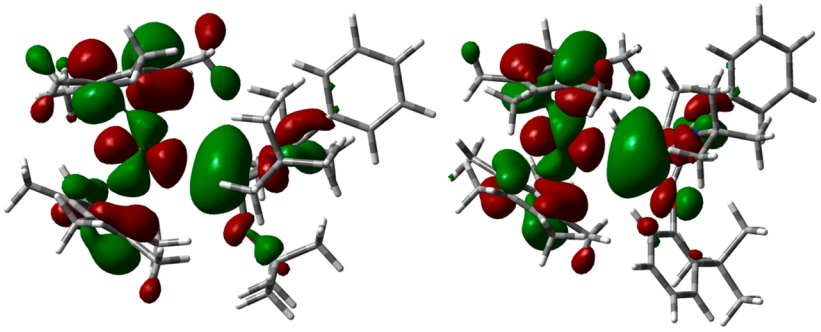

Figure 12. HOMOs of **5** and **6** (left and right, respectively) calculated at the B3PW91/Basis1 level of theory (isovalue: 0.02). White, gray, blue, turquoise, and teal refer to H, C, N, Sm, and Si atoms, respectively.

by a full-matrix least-squares method (*SHELXL97*).[73] If not noted otherwise, all non-H atoms were refined with anisotropic displacement parameters. All H atoms were located in calculated positions to correspond to standard bond lengths and angles. All diagrams were drawn with 30% probability thermal ellipsoids, and all H atoms were omitted for clarity. Crystallographic data (excluding structure factors) for the structures of compounds **2a**−**2d**, **3**, and **5**−**7** reported in this paper have been deposited with the Cambridge Crystallographic Data Centre as supplementary publications CCDC 1024428 (**2a**), 1024431 (**2b**), 1024432 (**2c**), 1024430 (**2d**), 1024429 (**3**), 1024433 (**5**), 1024434 (**6**), and 1024435 (**7**). Copies of these data can be obtained free of charge at http://www.ccdc.cam.ac.uk/products/csd/request/.

DFT Calculations. DFT calculations were carried out using the *Gaussian 09* program.[74] Geometry optimization was performed with the B3PW91 functional[75−77] because it was effectively applied for analog f-block element−carbene complexes.[78] We employed the Stuttgart RSC 1997 ECP[79] basis set from Basis Set Exchange[80,81] for f-block (lanthanide) elements, 6-31+G(d,p)[82] for Si atoms and 6-31G(d)[83,84] basis for the other atoms, denoted as Basis1 in the paper. Natural population analysis was performed with *NBO program 5.0*,[85−87] implemented in *Gaussian 09*.

*Potassium (18-Crown-6)[1,4-(1,1,4,4-tetrakis(trimethylsilyl)-tetramethyltetrasilanylene]dicyclopentadienylthuliate (**2a**).* A suspension of Cp_3Tm (98 mg, 0.27 mmol) in toluene (5 mL) was added dropwise to a solution of **1** (310 mg, 0.29 mmol) in THF (4 mL). After 1 h of stirring, the reaction mixture turned into a clear yellow solution and was treated with pentane (8 mL). Yellow crystals of **2a** (387 mg, 93%) were obtained after 16 h at room temperature. Mp: 264−268 °C. HR ESI-MS. Calcd for $C_{26}H_{58}TmO_2Si_8$: m/z 795.1935. Found: m/z 795.1928. ^{1}H NMR (THF-d_8): δ 16.7 (s, 36H, $SiMe_3$), 5.1 (s, 5H, Cp), 2.5 (s, 48H, 18-cr-6), −11.9 (s, 12H, $SiMe_2$), −48.3 (s, 10H, Cp). ^{13}C{^{1}H} NMR (THF-d_8): δ 70.3 (18-cr-6), 7.6 ($SiMe_3$), not detected ($SiMe_2$), not detected (Cp signals). ^{29}Si{^{1}H} NMR (THF-d_8): δ −5.2 ($SiMe_3$), −26.6 ($SiMe_2$), not detected (Si_q).

*Potassium (18-Crown-6)[1,4-(1,1,4,4-tetrakis(trimethylsilyl)-tetramethyltetrasilanylene]dicyclopentadienylholmiate (**2b**).* The same procedure as that for **2a** was used except with **1** (268 mg, 0.25 mmol) and Cp_3Ho (90 mg, 0.25 mmol). Orange crystals of **2b** (210 mg, 59%) were obtained after 2 days at −60 °C. Mp: 155−160 °C. HR ESI-MS. Calcd for $C_{26}H_5HoO_2Si_8$: m/z 791.1904. Found: m/z 791.1889. ^{1}H NMR (THF-d_8): δ 6.89 (s, 5H, Cp), 4.26 (s, 48H, 18-cr-6), 1.67 (s, 12H, $SiMe_2$), 1.58 (s, 36H, $SiMe_3$), −22.42 (s, 10H, Cp). ^{13}C{^{1}H} NMR (THF-d_8): δ 71.6 (18-cr-6), 3.4 ($SiMe_3$), −0.1 ($SiMe_2$), not detected (Cp signals). ^{29}Si{^{1}H} NMR (THF-d_8): δ −9.0 ($SiMe_3$), −35.2 ($SiMe_2$), −114.9 (Si_q). UV/vis (Et_2O): λ_1 = 253 nm and $\varepsilon_1 = 2.8 \times 10^4$ L mol^{-1} cm^{-1}; λ_2 = 283 nm and $\varepsilon_2 = 6.2 \times 10^3$ L mol^{-1} cm^{-1}; λ_3 = 342 nm and $\varepsilon_3 = 3.2 \times 10^3$ L mol^{-1} cm^{-1}.

*Potassium (18-Crown-6)[1,4-(1,1,4,4-tetrakis(trimethylsilyl)-tetramethyltetrasilanylene]dicyclopentadienylterbiate (**2c**).* The same procedure as that for **2a** was used except with **1** (353 mg, 0.33 mmol) and $TbCp_3$ (116 mg, 0.33 mmol). Yellow crystals of **2d** (301 mg, 64%) were obtained after 2 days at −35 °C. Mp: 183−186 °C. ^{1}H NMR (THF-d_8): δ 5.72 (s, 5H, Cp), 2.50 (s, 48H, 18-cr-6), 0.72 (s, 12H, $SiMe_2$), 0.63 (s, 36H, $SiMe_3$), −24.32 (s, 10H, Cp). ^{13}C{^{1}H} NMR (THF-d_8): δ 69.9 (18-cr-6), 3.6 ($SiMe_3$), not detected ($SiMe_2$), not detected (Cp signals). ^{29}Si{^{1}H} NMR (THF-d_8): δ −10.6 ($SiMe_3$), −36.1 ($SiMe_2$), −116.3 (Si_q).

*Potassium (18-Crown-6)[1,4-(1,1,4,4-tetrakis(trimethylsilyl)-tetramethyltetrasilanylene]dicyclopentadienylgadolinate (**2d**).* The same procedure as for that **2a** was used except for **1** (321 mg, 0.30 mmol) and $GdCp_3$ (106 mg, 0.30 mmol). Yellow crystals of **2c** (137 mg, 32%) were obtained after 2 days at −60 °C. Mp: 172−175 °C. HR ESI-MS. Calcd for $C_{26}H_{58}GdO_2Si_8$: m/z 784.1833. Found: m/z 784.1826. ^{1}H NMR (THF-d_8): δ 9.23 (s, 10H, Cp), 7.85 (s, 5H, Cp), 4.40 (s, 18-cr-6), 2.35 (s, 36H, $SiMe_3$), 2.20 (s, 12H, $SiMe_2$). ^{13}C{^{1}H} NMR (THF-d_8): no signals detected. ^{29}Si{^{1}H} NMR (THF-d_8): δ −1.4 ($SiMe_2$), −7.7 ($SiMe_3$), not detected (Si_q). UV/vis (Et_2O): λ_1 = 252 nm and $\varepsilon_1 = 3.8 \times 10^4$ L mol^{-1} cm^{-1}; λ_2 = 287 nm and $\varepsilon_2 = 1.1 \times 10^4$ L mol^{-1} cm^{-1}; λ_3 = 342 nm and $\varepsilon_3 = 3.2 \times 10^3$ L mol^{-1} cm^{-1}; λ_4 = 395 nm and $\varepsilon_4 = 9.4 \times 10^2$ L mol^{-1} cm^{-1}.

*Dipotassium (18-Crown-6)$_2$[μ-1,4-(1,1,4,4-tetrakis(trimethylsilyl)-tetramethyltetrasilanylene]bis(tricyclopentadienylcerate) (**3**).* The same procedure as that for **2a** was used except with **1** (160 mg, 0.15 mmol) and $CeCp_3$ (100 mg, 0.30 mmol). Very sensitive yellow crystals of **3** (208 mg, 79%), suitable for single-crystal XRD analysis, were obtained after 16 h at room temperature.

Cp$_2$Sm ← :Si(OtBu){(NtBu)$_2$CPh} (**5**).* A Schlenk tube was charged with $Cp^*_2Sm(OEt_2)$ (0.173 g, 0.351 mmol) and ligand **4b** (0.117 g, 0.351 mmol). A total of 10 mL of degassed toluene was recondensed onto this solid mixture by submersion thereof in a liquid-nitrogen cold trap, under a static vacuum. After the recondensation was complete, the solvent was degassed once more upon thawing and allowed to slowly warm to room temperature with rapid stirring. Upon warming to room temperature, the reaction solution had a dark-green appearance. After stirring for 3 h at room temperature, an in situ ^{1}H NMR spectrum of the reaction solution revealed the selective formation of a new product. The reaction solution was concentrated in vacuo under reduced pressure to ca. 2 mL and cooled to −30 °C for 1 h to complete the precipitation of the product. The light-green supernatant was removed by cannula filtration at −50 °C, and the remaining emerald-green solid was dried in vacuo for 1 h at a pressure of 3×10^{-2} mbar. (Crystals of the dinuclear complex **7** were obtained from the light-green supernatant solution as a trace byproduct and structurally characterized by single-crystal XRD analysis.) The product was afforded as **5**·toluene (0.189 g, 71%). Mp: 158−161 °C. HR ESI-MS: no signal for $[M + H]^+$ observed; $[\mathbf{4b} + H]^+$ observed with matching isotope pattern. Calcd for $C_{19}H_{32}N_2OSi$: m/z 333.2357. Found: m/z 333.2358. Magnetic moment (Evans' method, 8 mg mL^{-1}, 298 K, C_6D_6): μ_{eff} = 2.6 μ_B. ^{1}H NMR (benzene-d_6, 40 mg mL^{-1}): δ 6.97−7.14 (m, 5H, Ar−*H*, toluene), 6.36 (t, 1H, Ph), 6.19 (d, 1H, Ph), 6.10 (ps t, 1H, Ph), 4.80 (br, 1H, Ph), 4.31 (br s, 18H, N*t*Bu), 3.69 (br s, 30H, 2Cp*), 2.38 (br, 1H, Ph), 2.11 (s, 3H, toluene), 0.91 (s, 9H, O*t*Bu). ^{13}C{^{1}H} NMR (benzene-d_6, 40 mg mL^{-1}): NCN not visible, δ 159.2 (s, C^1, Ph), 137.9 (s, toluene), 129.3 (s, toluene), 128.9 (s, toluene), 127.4 (s, Ph), 125.6 (s, toluene), 124.1 (s, Ph), 119.6 (s, Ph). 118.9 (s, Ph), 115.1 (br s, Ph), 101.9 (v br, 2C_5Me_5), 55.9 (s, 2$NCMe_3$), 38.9 (s, $OCMe_3$), 30.8 (s, 2$NCMe_3$), 21.4 (s, CH_3, toluene), signals for C_5Me_5 and $OCMe_3$ not detected. ^{29}Si{^{1}H} NMR (benzene-

DOI: 10.1021/ic502991p
Inorg. Chem. 2015, 54, 3306−3315

d_6, 40 mg mL^{-1}): no signal observed even at very high concentrations and >72 h data acquisition time.

Cp$^*_2$Sm ← :Si(O−C$_6$H$_4$-2-tBu){(NtBu)$_2$CPh}* (**6**). A procedure similar to that in the preparation of complex **7** was employed: A Schlenk tube was charged with Cp*$_2$Sm(OEt$_2$) (0.181 g, 0.367 mmol) and ligand **4a** (0.150 g, 0.367 mmol). A total of 10 mL of degassed toluene was recondensed onto this solid mixture by submersion thereof in a liquid-nitrogen cold trap, under static vacuum. After the recondensation was complete, the solvent was degassed once more upon thawing and allowed to slowly warm to room temperature with rapid stirring. Upon warming to room temperature, the reaction solution had a dark-green appearance. After stirring for 3 h at room temperature, an in situ ^{1}H NMR spectrum of the reaction solution revealed the selective formation of a new product. The reaction solution was concentrated in vacuo under reduced pressure to ca. 2 mL and cooled to −30 °C for 1 h to complete the precipitation of the product. A light-brown supernatant was removed by cannula filtration at −50 °C, and the remaining emerald-green solid was dried in vacuo for 1 h at a pressure of 3 × 10^{-2} mbar. The product was afforded as **6** (0.177 g, 55%). Mp: 164−166 °C. HR ESI-MS. Calcd for $C_{45}H_{66}N_2O_3SiSm$: m/z 862.4043. Found: m/z 862.4023 ([M + H + O$_2$]$^+$). Magnetic moment (Evans' method, 8 mg mL^{-1}, 298 K, C_6D_6): μ_{eff} = 2.7 μ_B. EPR (30 K, pentane solution microwave frequency 9.476 GHz, power 2 mW, modulation amplitude 0.5 mT): g_{iso} = 2.15. ^{1}H NMR (benzene-d_6, 40 mg mL^{-1}): δ 10.90 (br s, 1H, OAr), 9.57 (br s, 1H, OAr), 7.28 (d, 2H, OAr), 7.21 (t, 1H, Ph), 6.97 (ps quart, 1H, Ph), 6.82 (t, 1H, Ph), 6.34 (t, 1H, Ph), 5.68 (d, 1H, Ph), 3.43 (br s, 18H, N*t*Bu), 2.29 (br s, 30H, 2Cp*), 1.27 (br, 9H, Ar−*t*Bu). ^{13}C{^{1}H} NMR (benzene-d_6, 40 mg mL^{-1}): δ 165.2 (br s, NCN), 155.4 (br s, C^1, OAr), 142.5 (s, C^1, Ph), 138.2 (br s, Ar), 137.5 (s, Ar), 134.7 (s, Ar), 134.4 (s, Ar), 130.3 (s, Ar), 129.9 (s, Ar), 127.1 (s, Ar), 121.0 (br s, Ar), 120.4 (br s, Ar), 118.7 (s, Ar), 101.9 (v br, 2C$_5$*Me*$_5$), 55.9 (v br s, 2NCMe$_3$ + Ar−C*Me*$_3$), 36.7 (s, Ar−C*Me*$_3$), 30.8 (s, 2NC*Me*$_3$), signals for C_5Me_5. ^{29}Si{^{1}H} NMR (benzene-d_6, 40 mg mL^{-1}): no signal observed even at very high concentrations and >72 h data acquisition time.

■ ASSOCIATED CONTENT

Ⓢ Supporting Information

X-ray crystallographic data in CIF format, details of the XRD studies, EPR, ESI-MS, and UV/vis spectra, tables of Cartesian coordinates, and absolute energies for all of the complexes studied. This material is available free of charge via the Internet at http://pubs.acs.org.

■ AUTHOR INFORMATION

Corresponding Authors

*E-mail: szilvasitibor@ch.bme.hu.
*E-mail: burgert.blom@tu-berlin.de.
*E-mail: baumgartner@tugraz.at.

Notes

The authors declare no competing financial interest.

■ ACKNOWLEDGMENTS

B.B. thanks the UniCat Cluster of Excellence for financial support and Prof. Dr. Matthias Driess for useful discussions and the space to pursue independent work. D. Gallego and S. Yao (Technische Universität Berlin) are also thanked for some experimental assistance and Dr. M. van Gastel (MPI f. Chem. Energiekonversion, Mülheim) is thanked for recording the EPR spectrum of complex **6**. Support for this study was provided by the Austrian Fonds zur Förderung der wissenschaftlichen Forschung via Project P-25124 (to J.B.). T.S. is thankful for generous support by The New Széchenyi Plan TÁMOP-4.2.2/B-10/1-2010-0009.

■ REFERENCES

(1) Liddle, S. T.; Mills, D. P. *Dalton Trans.* **2009**, 5592−5605.
(2) Edelmann, F. T. *Coord. Chem. Rev.* **2006**, *250*, 2511−2564.
(3) Edelmann, F. T. *Coord. Chem. Rev.* **2012**, *256*, 1151−1228.
(4) Bochkarev, L. N.; Makarov, V. M.; Hrzhanovskaya, Y. N.; Zakharov, L. N.; Fukin, G. K.; Yanovsky, A. I.; Struchkov, Y. T. *J. Organomet. Chem.* **1994**, *467*, C3−C5.
(5) Schumann, H.; Nickel, S.; Hahn, E.; Heeg, M. J. *Organometallics* **1985**, *4*, 800−801.
(6) Schumann, H.; Meese-Marktscheffel, J. A.; Hahn, F. E. *J. Organomet. Chem.* **1990**, *390*, 301−308.
(7) Schumann, H.; Nickel, S.; Loebel, J.; Pickardt, J. *Organometallics* **1988**, *7*, 2004−2009.
(8) Sgro, M. J.; Piers, W. E. *Inorg. Chim. Acta* **2014**, *422*, 243−250.
(9) Campion, B. K.; Heyn, R. H.; Tilley, T. D. *Organometallics* **1993**, *12*, 2584−2590.
(10) Corradi, M. M.; Frankland, A. D.; Hitchcock, P. B.; Lappert, M. F.; Lawless, G. A. *Chem. Commun.* **1996**, 2323−2324.
(11) Hou, Z.; Zhang, Y.; Nishiura, M.; Wakatsuki, Y. *Organometallics* **2003**, *22*, 129−135.
(12) Radu, N. S.; Tilley, T. D.; Rheingold, A. L. *J. Am. Chem. Soc.* **1992**, *114*, 8293−8295.
(13) Radu, N. S.; Tilley, T. D.; Rheingold, A. L. *J. Organomet. Chem.* **1996**, *516*, 41−49.
(14) Radu, N. S.; Tilley, T. D. *J. Am. Chem. Soc.* **1995**, *117*, 5863−5864.
(15) Radu, N. S.; Hollander, F. J.; Tilley, T. D.; Rheingold, A. L. *Chem. Commun.* **1996**, 2459−2460.
(16) Gossage, R. A. *J. Organomet. Chem.* **2000**, *608*, 164−171.
(17) Castillo, I.; Tilley, T. D. *Organometallics* **2000**, *19*, 4733−4739.
(18) Perrin, L.; Maron, L.; Eisenstein, O.; Tilley, T. D. *Organometallics* **2009**, *28*, 3767−3775.
(19) Castillo, I.; Tilley, T. D. *Organometallics* **2001**, *20*, 5598−5605.
(20) Cai, X.; Gehrhus, B.; Hitchcock, P. B.; Lappert, M. F. *Can. J. Chem.* **2000**, *78*, 1484−1490.
(21) Evans, W. J.; Perotti, J. M.; Ziller, J. W.; Moser, D. F.; West, R. *Organometallics* **2003**, *22*, 1160−1163.
(22) Arp, H.; Zirngast, M.; Marschner, C.; Baumgartner, J.; Rasmussen, K.; Zark, P.; Müller, T. *Organometallics* **2012**, *31*, 4309−4319.
(23) Zirngast, M.; Flörke, U.; Baumgartner, J.; Marschner, C. *Chem. Commun.* **2009**, 5538−5540.
(24) Kayser, C.; Kickelbick, G.; Marschner, C. *Angew. Chem., Int. Ed.* **2002**, *41*, 989−992.
(25) Fischer, R.; Frank, D.; Gaderbauer, W.; Kayser, C.; Mechtler, C.; Baumgartner, J.; Marschner, C. *Organometallics* **2003**, *22*, 3723−3731.
(26) Birmingham, J. M.; Wilkinson, G. *J. Am. Chem. Soc.* **1956**, *78*, 42−44.
(27) Berg, D. J.; Burns, C. J.; Andersen, R. A.; Zalkin, A. *Organometallics* **1989**, *8*, 1865−1870.
(28) Blom, B.; Stoelzel, M.; Driess, M. *Chem.—Eur. J.* **2013**, *19*, 40−62.
(29) So, C.-W.; Roesky, H. W.; Magull, J.; Oswald, R. B. *Angew. Chem., Int. Ed.* **2006**, *45*, 3948−3950.
(30) Sen, S. S.; Roesky, H. W.; Stern, D.; Henn, J.; Stalke, D. *J. Am. Chem. Soc.* **2010**, *132*, 1123−1126.
(31) Sen, S. S.; Jana, A.; Roesky, H. W.; Schulzke, C. *Angew. Chem., Int. Ed.* **2009**, *48*, 8536−8538.
(32) Azhakar, R.; Roesky, H. W.; Ghadwal, R. S.; Holstein, J. J.; Dittrich, B. *Dalton Trans.* **2012**, *41*, 9601−9603.
(33) Blom, B.; Klatt, G.; Gallego, D.; Tan, G.; Driess, M. *Dalton Trans.* **2015**, *44*, 639−644.
(34) Evans, D. F. *J. Chem. Soc.* **1959**, 2003−2005.
(35) Sharp, R. R. *Nucl. Magn. Reson.* **2003**, *32*, 473−519.
(36) Kime, K. A.; Sievers, R. E. *Aldrichimica Acta* **1977**, *10*, 54−62.
(37) Ammon, R.; Kanellakopulos, B.; Fischer, R. D.; Laubereau, P. *Inorg. Nucl. Chem. Lett.* **1969**, *5*, 315−319.
(38) Eggers, S. H.; Hinrichs, W.; Kopf, J.; Jahn, W.; Fischer, R. D. *J. Organomet. Chem.* **1986**, *311*, 313−323.

DOI: 10.1021/ic502991p
Inorg. Chem. 2015, 54, 3306−3315

(39) Jaroschik, F.; Nief, F.; Ricard, L. *Chem. Commun.* **2006**, 426−428.
(40) Evans, W. J.; Allen, N. T.; Ziller, J. W. *Angew. Chem., Int. Ed.* **2002**, *41*, 359−361.
(41) Nief, F.; de Borms, B. T.; Ricard, L.; Carmichael, D. *Eur. J. Inorg. Chem.* **2005**, 637−643.
(42) Jaroschik, F.; Nief, F.; Le Goff, X.-F.; Ricard, L. *Organometallics* **2007**, *26*, 3552−3558.
(43) Schumann, H.; Glanz, M.; Hemling, H. *J. Organomet. Chem.* **1993**, *445*, C1−C3.
(44) MacDonald, M. R.; Bates, J. E.; Ziller, J. W.; Furche, F.; Evans, W. J. *J. Am. Chem. Soc.* **2013**, *135*, 9857−9868.
(45) Schumann, H.; Esser, L.; Loebel, J.; Dietrich, A.; Van der Helm, D.; Ji, X. *Organometallics* **1991**, *10*, 2585−2592.
(46) Song, S.; Shen, Q.; Jin, S.; Guan, J.; Lin, Y. *Polyhedron* **1992**, *11*, 2857−2861.
(47) Xie, Z.; Wang, S.; Zhou, Z.-Y.; Mak, T. C. W. *Organometallics* **1999**, *18*, 1641−1652.
(48) Xie, Z.; Chui, K.; Yang, Q.; Mak, T. C. W.; Sun, J. *Organometallics* **1998**, *17*, 3937−3944.
(49) Shen, H.; Chan, H.-S.; Xie, Z. *Organometallics* **2008**, *27*, 5309−5316.
(50) Layfield, R. A.; Bashall, A.; McPartlin, M.; Rawson, J. M.; Wright, D. S. *Dalton Trans.* **2006**, 1660−1666.
(51) Evans, W. J.; Bloom, I.; Hunter, W. E.; Atwood, J. L. *J. Am. Chem. Soc.* **1981**, *103*, 6507−6508.
(52) Baisch, U.; Pagano, S.; Zeuner, M.; Barros, N.; Maron, L.; Schnick, W. *Chem.—Eur. J.* **2006**, *12*, 4785−4798.
(53) Baisch, U.; Pagano, S.; Zeuner, M.; Schmedt auf der Günne, J.; Oeckler, O.; Schnick, W. *Organometallics* **2006**, *25*, 3027−3033.
(54) Wu, Z.; Xu, Z.; You, X.; Wang, H.; Zhou, X. *Polyhedron* **1993**, *12*, 677−681.
(55) Schulz, H.; Schultze, H.; Reddmann, H.; Link, M.; Amberger, H.-D. *J. Organomet. Chem.* **1992**, *424*, 139−152.
(56) Schmitz, J.; Schilder, H.; Lueken, H. *J. Alloys Compd.* **1994**, *209*, 49−58.
(57) Sun, Y.; Zhang, Z.; Wang, X.; Li, X.; Weng, L.; Zhou, X. *Dalton Trans.* **2009**, *39*, 221−226.
(58) Zhang, J.; Zhou, X.; Cai, R.; Weng, L. *Inorg. Chem.* **2005**, *44*, 716−722.
(59) Pernin, C. G.; Ibers, J. A. *Inorg. Chem.* **2000**, *39*, 1216−1221.
(60) Evans, W. J.; Deming, T. J.; Ziller, J. W. *Organometallics* **1989**, *8*, 1581−1583.
(61) Gradeff, P. S.; Yunlu, K.; Deming, T. J.; Olofson, J. M.; Ziller, J. W.; Evans, W. J. *Inorg. Chem.* **1989**, *28*, 2600−2604.
(62) Cordero, B.; Gómez, V.; Platero-Prats, A. E.; Revés, M.; Echeverría, J.; Cremades, E.; Barragán, F.; Alvarez, S. *Dalton Trans.* **2008**, 2832−2838.
(63) Perrin, L.; Maron, L.; Eisenstein, O. *Faraday Discuss.* **2003**, *124*, 25−39.
(64) Evans, W. J.; Grate, J. W.; Levan, K. R.; Bloom, I.; Peterson, T. T.; Doedens, R. J.; Zhang, H.; Atwood, J. L. *Inorg. Chem.* **1986**, *25*, 3614−3619.
(65) Evans, W. J.; Drummond, D. K.; Hughes, L. A.; Zhang, H.; Atwood, J. L. *Polyhedron* **1988**, *7*, 1693−1703.
(66) Evans, W. J.; Perotti, J. M.; Kozimor, S. A.; Champagne, T. M.; Davis, B. L.; Nyce, G. W.; Fujimoto, C. H.; Clark, R. D.; Johnston, M. A.; Ziller, J. W. *Organometallics* **2005**, *24*, 3916−3931.
(67) Pangborn, A. B.; Giardello, M. A.; Grubbs, R. H.; Rosen, R. K.; Timmers, F. J. *Organometallics* **1996**, *15*, 1518−1520.
(68) Morris, G. A.; Freeman, R. *J. Am. Chem. Soc.* **1979**, *101*, 760−762.
(69) Helmer, B. J.; West, R. *Organometallics* **1982**, *1*, 877−879.
(70) *SAINTPLUS: Software Reference Manual*, version 6.45; Bruker-AXS Inc.: Madison, WI, 1997−2003.
(71) Blessing, R. H. *Acta Crystallogr., Sect. A* **1995**, *51*, 33−38.
(72) Sheldrick, G. M. *SADABS*, version 2.10; Bruker AXS Inc.: Madison, WI, 2003.
(73) Sheldrick, G. M. *Acta Crystallogr., Sect. A* **2007**, *64*, 112−122.
(74) Frisch, M. J.; Trucks, G. W.; Cheeseman, J. R.; Scalmani, G.; Caricato, M.; Hratchian, H. P.; Li, X.; Barone, V.; Bloino, J.; Zheng, G.; Vreven, T.; Montgomery, J. A.; Petersson, G. A.; Scuseria, G. E.; Schlegel, H. B.; Nakatsuji, H.; Izmaylov, A. F.; Martin, R. L.; Sonnenberg, J. L.; Peralta, J. E.; Heyd, J. J.; Brothers, E.; Ogliaro, F.; Bearpark, M.; Robb, M. A.; Mennucci, B.; Kudin, K. N.; Staroverov, V. N.; Kobayashi, R.; Normand, J.; Rendell, A.; Gomperts, R.; Zakrzewski, V. G.; Hada, M.; Ehara, M.; Toyota, K.; Fukuda, R.; Hasegawa, J.; Ishida, M.; Nakajima, T.; Honda, Y.; Kitao, O.; Nakai, H. *Gaussian 09*; Gaussian Inc.: Wallingford, CT, 2009.
(75) Perdew, J. P. In *Electronic Structure of Solids '91*; Ziesche, P., Eschrig, H., Eds.; Akademie Verlag: Berlin, 1991; pp 11−20.
(76) Becke, A. D. *J. Chem. Phys.* **1993**, *98*, 5648−5652.
(77) Burke, K.; Perdew, J. P.; Wang, Y. In *Electronic density functional theory: recent progress and new directions*; Dobson, J. F., Vignale, G., Das, M. P., Eds.; Plenum Press: New York, 1998; pp 81−111.
(78) Maron, L.; Bourissou, D. *Organometallics* **2007**, *26*, 1100−1103.
(79) Dolg, M.; Stoll, H.; Savin, A.; Preuss, H. *Theor. Chim. Acta* **1989**, *75*, 173−194.
(80) Feller, D. *J. Comput. Chem.* **1996**, *17*, 1571−1586.
(81) Schuchardt, K. L.; Didier, B. T.; Elsethagen, T.; Sun, L.; Gurumoorthi, V.; Chase, J.; Li, J.; Windus, T. L. *J. Chem. Inf. Model.* **2007**, *47*, 1045−1052.
(82) Clark, T.; Chandrasekhar, J.; Spitznagel, G. W.; Schleyer, P. V. R. *J. Comput. Chem.* **1983**, *4*, 294−301.
(83) Hariharan, P. C.; Pople, J. A. *Theor. Chim. Acta* **1973**, *28*, 213−222.
(84) Frisch, M. J.; Pople, J. A.; Binkley, J. S. *J. Chem. Phys.* **1984**, *80*, 3265−3269.
(85) Glendening, E. D.; Badenhoop, J. K.; Reed, A. E.; Carpenter, J. E.; Bohman, J. A.; Morales, C. M.; Weinhold, F. *NBO*, version 5.0; NBO: Madison, WI, 2001.
(86) Weinhold, F.; Landis, C. R. *Chem. Educ. Res. Pract.* **2001**, *2*, 91−104.
(87) Carpenter, J. E.; Weinhold, F. *J. Mol. Struct.: THEOCHEM* **1988**, *169*, 41−62.

DOI: 10.1021/ic502991p
Inorg. Chem. 2015, 54, 3306−3315